CrystEngComm

COMMUNICATION

View Article Online
View Journal | View Issue

Cite this: *CrystEngComm*, 2016, **18**, 7430

Received 11th July 2016,
Accepted 18th August 2016

DOI: 10.1039/c6ce01536k

www.rsc.org/crystengcomm

Selective growth of silver particles on the facets of synthetic diamond†

B. B. Bokhonov*[ab] and H. Kato[c]

We have shown for the first time that simple annealing of silver–synthetic diamond mixtures in air or oxygen at 600–700 °C leads to selective growth of silver particles on the {100} facets of diamond, while no growth is observed on the {111} facets. Annealing at a temperature higher than 750 °C results in significant morphological changes in the heterostructure: silver particles grow not only on the cube but also on the octahedral facets.

The unique properties of diamond – unbeatable hardness, high wear resistance and high thermal conductivity – make it an indispensable material for the manufacturing and electronic industries.[1] The development of the production methods of synthetic diamonds has reduced their cost, widening their applications as components of a variety of functional materials.

It is well known that the physical and chemical properties of composite materials depend on the structure of interfaces between the components.[2] In order to improve the functional properties of the diamond-containing materials by establishing an intimate contact between the phases, methods of surface modification of diamond crystals are being developed. Within a wide spectrum of diamond-based composite materials and heterostructures, metal–diamond systems attract the most attention. Studies of metal–diamond systems have revealed anisotropic etching of diamond facets by metals.[3] Extensive data on anisotropic etching of diamond by carbide-forming elements – Fe subgroup metals (Fe, Co, Ni) – have been collected over the past decade.[4] It was shown that the {100} planes etch faster than the {111} planes, while the etching rates of both sets of planes increase with temperature. It was also demonstrated that graphitization of diamond followed by diffusion of carbon into molten iron are the two main factors enabling the removal of carbon from the diamond surface.

Metal–diamond composites containing carbide-forming metals are obtained by solid state sintering, while those containing metals that do not form carbides and poorly wet the diamond surface are usually obtained by infiltration of metallic melts into porous diamond preforms.[5] In the latter, the contact between the metal matrix and the diamond crystals is improved by depositing titanium-, silicon-, tungsten- or chromium-based coatings on the diamond surface.[6]

By developing diamond–silver composites, it is possible to achieve unique combinations of thermal, optical, and antibacterial properties.[7] Understanding the underlying principles of the interface formation in the silver–diamond heterostructure is both scientifically challenging and technologically important. Therefore, the modification of diamond surfaces by silver in the absence of intermediate layers (interfacial coatings) and the elucidation of the interaction mechanisms are timely and relevant goals.

In the present work, we focused on the morphological and structural evolution of heterostructures consisting of metallic silver particles and micrometer-sized synthetic diamond crystals during annealing in air, argon and hydrogen. The preparation method of the silver–diamond heterostructures and the synthesis conditions are described in the experimental part of the ESI.†

The silver–diamond heterostructures were studied by scanning electron microscopy (SEM), X-ray diffraction (XRD) and energy-dispersive X-ray spectroscopy (EDS). Mass spectroscopy was used to monitor the changes in the system during the synthesis of the heterostructure.

Experiments have shown that morphological and structural features of the silver–diamond heterostructures that formed during annealing depend on the following parameters:

-temperature and duration of annealing;

[a] *Institute of Solid State Chemistry and Mechanochemistry SB RAS, Kutateladze str. 18, Novosibirsk, 630128, Russia. E-mail: bokhonov@solid.nsc.ru*
[b] *Novosibirsk State University, Pirogova str. 2, Novosibirsk, 630090, Russia*
[c] *Institute for Materials Research, Tohoku University, Aoba Ku, 2-1-1 Katahira, Sendai, Miyagi 9808577, Japan*

† Electronic supplementary information (ESI) available: Additional EDS spectra and SEM images. See DOI: 10.1039/c6ce01536k

-annealing atmosphere.

The most interesting features of the silver–diamond heterostructures were observed after annealing under an atmosphere of oxygen and in air. Fig. 1a shows an image of the diamond microcrystals. Diamond crystals of a similar morphology have been described in ref. 8. They have a cuboctahedral shape with mostly octahedral {111} and cube {100} facets developed. The XRD pattern of the diamond microcrystals shows the (111) and (220) reflections (Fig. 1b). By simply annealing the diamond crystals mixed with a silver powder (the overall composition of the mixture was 90 wt% Ag–10 wt% diamond) in air or under an atmosphere of oxygen for 10 min at 600–700 °C, it is possible to form diamond–silver heterostructures, in which silver particles with a size of 0.3–1 μm are preferentially located on the cube {100} diamond facets (Fig. 2a). Selective deposition of silver on the cube facets leaves only a few particles located on the octahedral {111} facets. The XRD patterns of the synthesized heterostructures contain the (111), (200), (220) and (311) reflections of metallic silver along with reflections of diamond (Fig. 2b). The EDS spectra of the heterostructures contain lines of carbon and silver (Fig. S1†). Fig. S2† shows elemental maps recorded to characterize the selective deposition of silver on a cube facet of diamond. With increasing annealing time of the silver–diamond mixture, the size and concentration of silver particles growing on the {100} diamond facets increase (Fig. 3a). Furthermore, when the annealing duration of the silver–diamond mixture reaches 1 h, oriented etching of the

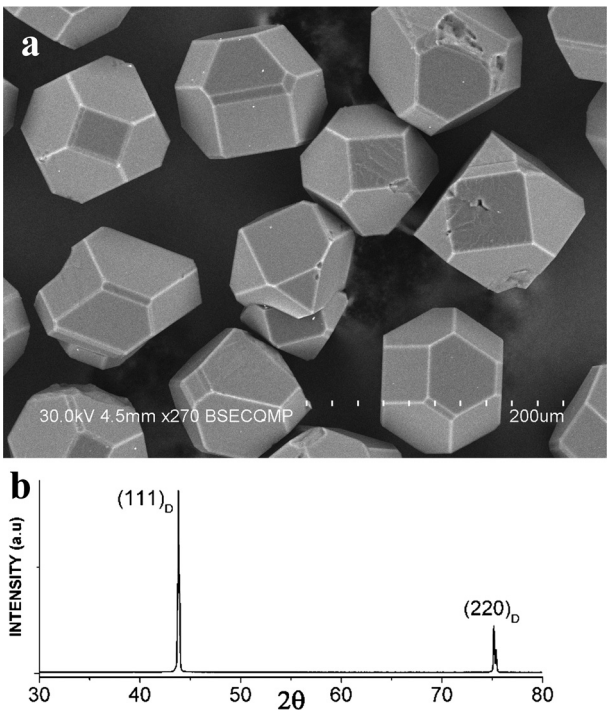

Fig. 1 (a) SEM image of the starting diamond crystals having a cuboctahedral shape with {100} and {111} facets. Additional SEM images of the diamond crystals can be found in the ESI.† (b) X-ray diffraction pattern of the starting diamond crystals.

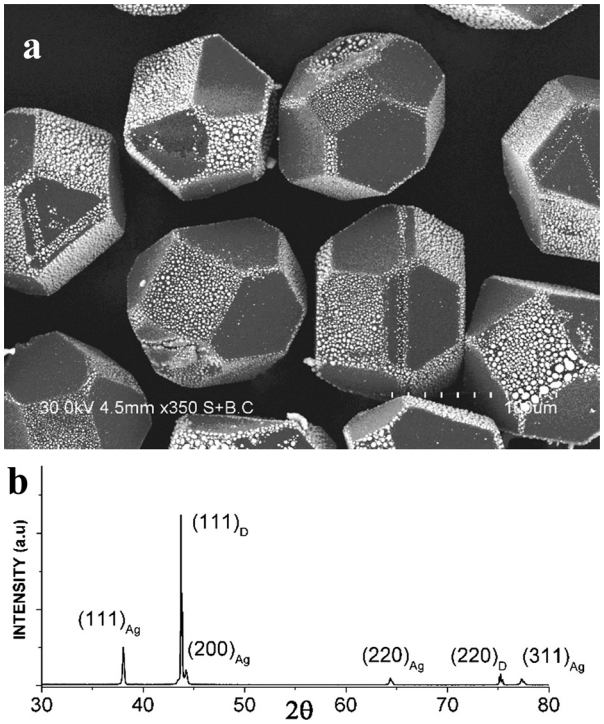

Fig. 2 (a) SEM image of Ag particles selectively deposited on the {100} facets of the diamond crystals during annealing in air at 700 °C. The {111} facets of the diamond crystals are consistently free from silver particles. Additional SEM images showing Ag/diamond crystals with plane selectivity of the deposition of silver particles can be found in the ESI.† (b) X-ray diffraction pattern of the Ag/diamond crystals annealed in air at 700 °C.

diamond surface occurs such that each silver particle is located in an etch pit. Treatment of these heterostructures by nitric acid results in dissolution of silver, revealing etch pits, which almost fully cover the {100} facets of the diamond microcrystals. The edges of these etch pits are parallel to the [110] and [1–10] crystallographic directions of diamond (Fig. 3b and S3†). There is a difference in the shape of the etch pits formed on the {100} facets of diamond by particles of carbide-forming metals[4] (Fe, Ni) and those formed by silver: while the former have a pyramidal shape, the latter have a flat bottom. Mass spectrometry has shown that upon heating of the mixture above 600 °C, evolution of a small amount of carbon dioxide (CO_2) occurs accompanied by a weight reduction of 0.05 wt%.

Annealing at a temperature of 750 °C leads to significant changes in the morphological features of the silver–diamond heterostructures. The silver particles appear to grow not only on the cube but also on the octahedral facets (Fig. 4a). However, a detailed study of the morphology and structure of the silver particles formed on the octahedral facets during annealing at 750 °C has shown that at this temperature, the {111} facets experience significant changes in their "crystallographic relief": many pyramidal etch pits form on their surface (Fig. 4b). The facets of these pits are the {100} planes, and it is these planes that silver particles grow on. Our

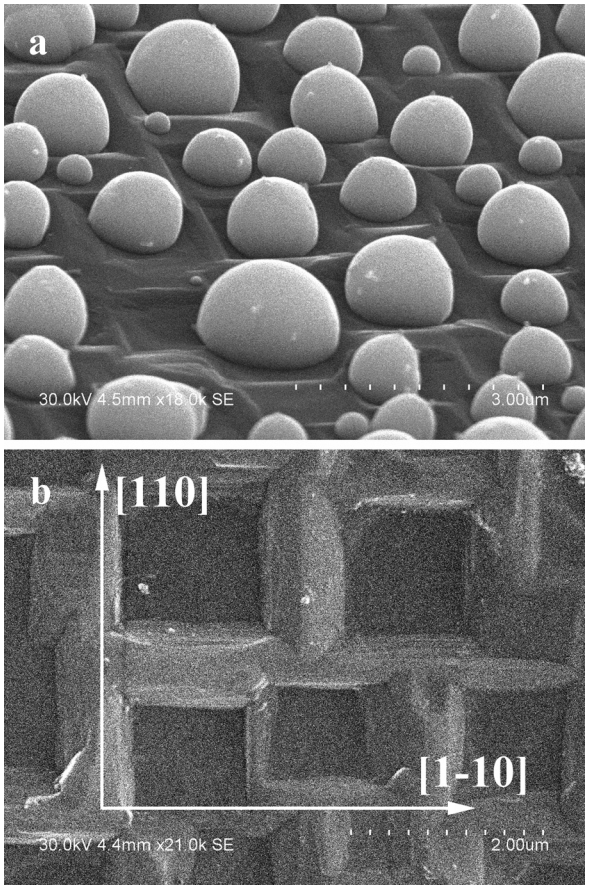

Fig. 3 (a) SEM image of silver particles on the (100) plane of diamond. Oriented etch pits are observed in the (100) facet, and silver particles are located in the corresponding etch pits. (b) SEM image of a (100) diamond facet after HNO_3 treatment. Additional low magnification SEM images showing the morphology of the Ag/diamond crystals after annealing and acid treatment can be found in the ESI.†

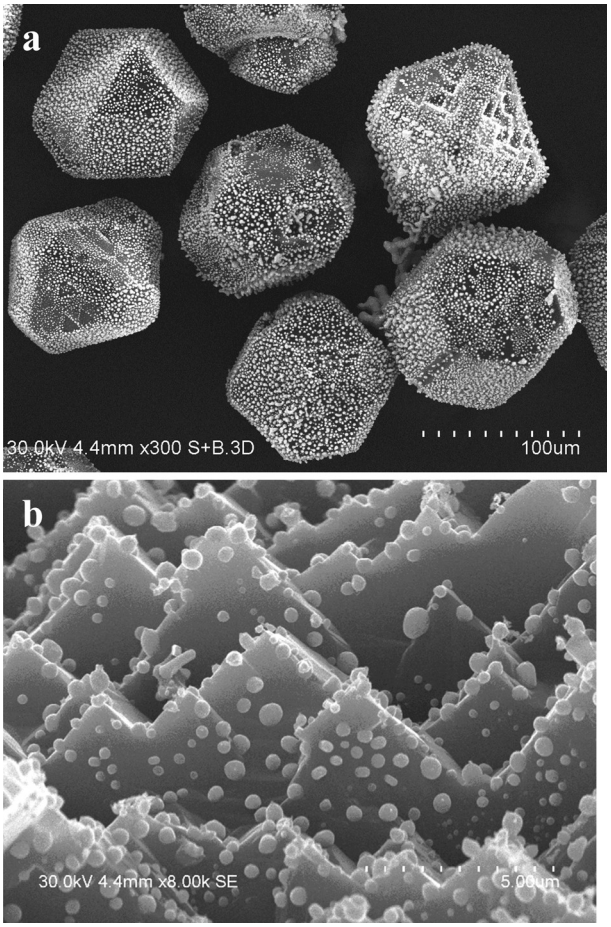

Fig. 4 (a) SEM image of Ag particles deposited on the diamond crystals during annealing in air at 750 °C. All diamond crystals having a cuboctahedral shape show Ag particles deposited on the {100} and {111} diamond planes. (b) Higher-magnification SEM image of an octahedral {111} diamond plane with deposited Ag particles. Many pyramidal etch pits form on the {111} surface.

experiments have shown that annealing of silver-free diamonds in air or oxygen leads to selective oxidative etching of the {111} facets and the formation of pyramidal etch pits (Fig. S4†), which agrees with the results reported in ref. 9.

We have found that silver particles can also deposit on the "octahedral" facets of the diamond microcrystals at temperatures below 700 °C, if the diamond crystals have been annealed at 750–800 °C prior to mixing and annealing with the silver powder (Fig. S5†).

It should be noted that selective deposition of particles on certain facets of crystals is used for the synthesis of a variety of materials.[10–16] At present, extensive research is aimed at developing the synthesis methods of heterostructures of various compositions, morphologies and structures. The widely known materials, whose faceted surface satisfies the requirements for the selective deposition of particles, are crystals of semiconducting oxides. The second component of these heterostructures is a noble metal that deposits selectively on certain facets of the semiconducting crystals.

For example, hybrid metal/Cu_2O nanostructures (metals = Cu, Au, Ag, Pt, Pd) have been prepared by galvanic reactions between Cu_2O and different metal salts or upon photoirradiation.[10] It was shown that the {111} surface of Cu_2O is much more facile to be reduced than the {110} and {100} surfaces. Using selective deposition, certain facets of TiO_2 were covered by Pt (ref. 12), Ag (ref. 13) and CdS (ref. 14) nanoparticles. It was found that Pt, PtNi and PtCo tips grow selectively on CdS nanorods.[15] An "inverse" system has also been obtained: ZnO nanoparticles were deposited on the surface of metallic silver.[16]

Selective deposition of Pt, Pd and Au nanoparticles on the surface of boron-doped polycrystalline diamond has been described in ref. 17. The deposition was conducted using an electrochemical method and from a nanoparticle-containing solution. The surface of diamond was subjected to treatment by hydrogen plasma and UV/ozone prior to deposition.[18]

The morphological features of the selective growth of silver particles on certain facets of diamond crystals observed in this work have similarities with the systems described above. However, there are also significant differences. Firstly, the previously known methods of selective deposition of particles

are based on the liquid-phase processes. In the present work, the deposition of silver on the {100} facets of diamond occurred while both components were remaining in the solid state. Indeed, the annealing temperature of the silver–diamond mixtures was much lower than the melting point of silver (T = 952 °C). Secondly, silver does not form carbides and there is virtually no mutual solubility in the Ag–C (graphite, amorphous carbon, diamond) system. Nonetheless, it was found that the growth of the silver particles of the {100} facets of diamond is accompanied by the formation of CO_2 gas.

An explanation of the selective growth of metallic particles on the facets of semiconducting crystals that is frequently provided is based on the difference in the surface energies of different facets of the crystal.[10–17] The selective growth of silver on diamond could have been explained in the same way. It is known that the surface energy of the {100} facets of diamond is substantially higher than that of the {111} facets.[18] If this energy-based explanation had been valid, similar selective deposition patterns of silver particles on the {100} facets of diamond would have been observed in experiments conducted under different atmospheres, *i.e.* no dependence of the selective deposition effect on the composition of the atmosphere would have been detected. However, our experiments have shown that during annealing of silver–diamond mixtures under hydrogen or argon atmosphere (Fig. S6†), no particle growth is observed on any diamond facet. This points to a specific role of oxygen in the process of selective deposition of silver on the {100} facets of diamond. Unfortunately, until now, the exact mechanism of diffusion of silver along the diamond surface in the presence of oxygen has not been elucidated, and investigations of the diamond–oxygen system are still continuing. It has been proven that the (111) facet is more reactive in the interaction with oxygen than the (100) facet.[9] During oxidation, the non-diamond carbon is removed from the (111) diamond facet faster than from the (100) facet. Recent experimental studies and theoretical calculations of the interaction of diamond with thermally activated and atomic oxygen confirmed the difference in the reactivity of the (111) and (100) diamond facets.[9c] In addition, it was found that the (100) surface, fully covered with ketones, is inert to carbon removal upon exposure to oxygen. The influence of oxygen on the selective deposition of metals on diamond facets was demonstrated in ref. 17*b*. The diamond crystals were subjected to ozone treatment for 10 s, and in contrast to our results, gold nanoparticles selectively deposited from a solution on the octahedral (111) facets of diamond. After treatment for 40–60 s, the gold nanoparticles deposited on the (100) facets as well. The effect of ozone treatment on the selective adsorption of gold nanoparticles on the treated diamond surface was explained by the removal of the non-diamond carbon layer prevailing for short treatment durations and oxidation of the diamond surface prevailing for long treatment durations.

In ref. 19, the etching process of diamond-like carbon (DLC) films by cold oxygen plasma in the presence of silver nanoparticles was studied. In contrast to our observations, which showed that in the presence of silver, etching of diamond occurs, DLC films were more wear resistant to etching when a greater number of silver nanoparticles were deposited on their surface. The authors suggested that silver nanoparticles present on the DLC films prevented the reaction of oxygen with carbon due to a higher reaction affinity of silver to oxygen atoms forming a silver oxide layer on the DLC surface under irradiation by the oxygen plasma.

Structural investigations of an amorphous carbon film containing silver nanoparticles in the presence of atomic oxygen showed that the diffusion rate of silver increases when the film is UV-irradiated.[20] The authors explained this effect by an increase in the concentration of the sp^2 carbon on the film surface.

The specific role of oxygen in the behavior of the Ag–C system is presented in ref. 21. It was shown that during annealing of mono- and multilayer graphenes, on which silver nanoparticles were deposited, a silver nanoparticle located at a graphene edge catalyzed the oxidation of neighboring carbon atoms, thereby burning a trench into the graphene layer. It is likely that the etching mechanism of the {100} facets by the growing silver particles observed in the present work is similar to that operating during catalytic oxidation of graphene.

The analysis of the literature data presented above shows that during interaction with oxygen, diamond facets with different indices develop different morphological characteristics and show different chemical compositions (in terms of the presence of functional groups) and structures (in terms of the presence of a non-diamond carbon layer). All these factors can affect the process of selective deposition of silver particles on the diamond surface during oxidative annealing demonstrated in this work. In order to unambiguously determine the reasons of the selective deposition of silver on the (100) facets of diamond, further investigations should be conducted, and answers to the following questions should be found:

How does silver from a separate particle diffuse across the surface of a diamond crystal to be deposited on its {100} facets?

Does the defect structure of diamond influence the selective deposition process? Can a possible difference in the charge state of different facets of diamond (ref. 22) influence the localization of the deposited silver?

What is the role of oxygen in the growth of silver particles? The effect of oxygen on both the surface structure/properties of different diamond facets and the charge state of silver particles should be elaborated.

The observed selective deposition of silver particles on the {100} facets of diamond can be used directly for the preparation of silver–diamond functional materials. Furthermore, conclusions derived from this study can be extended to other systems composed of non-metal micrometer-sized crystals and metal or alloy particles, for which annealing under different atmospheres can tailor the deposition selectivity of metallic particles onto the surface of the microcrystals.

In summary, we have shown for the first time that annealing of silver–synthetic diamond mixtures in air or oxygen results in the selective growth of silver particles on the {100} facets of diamond, while no growth is observed on the {111} facets. Due to simplicity and high facet selectivity, annealing-assisted deposition of particles on certain facets of micrometer-sized diamond crystals can be suggested as a versatile method for the preparation of different diamond-containing heterostructures.

References

1 (*a*) W. J. Zong, D. Li, T. Sun, K. Cheng and Y. C. Liang, *Int. J. Mach. Tool Manu.*, 2007, **47**, 864–871; (*b*) W. J. Zong, Z. Q. Li, T. Sun, K. Cheng, D. Li and S. Dong, *Int. J. Mach. Tool Manu.*, 2010, **50**(4), 411–419; (*c*) M. N. Touzelbaev and K. E. Goodson, *Diamond Relat. Mater.*, 1998, **7**(1), 1–14.

2 M. H. Huang, S. Rej and S.-C. Hsu, *Chem. Commun.*, 2014, **50**, 1634–1644.

3 (*a*) W. Tillmann, M. Ferreira, A. Steffen, K. Rüster, J. Möller, S. Bieder, M. Paulus and M. Tolan, *Diamond Relat. Mater.*, 2013, **38**, 118–123; (*b*) H.-A. Mehedi, C. Hebert, S. Ruffinatto, D. Eon, F. Omnes and E. Gheeraert, *Nanotechnology*, 2012, **23**, 455302, (7 pp); (*c*) S. Konishi, T. Ohashi, W. Sugimoto and Y. Takasu, *Chem. Lett.*, 2006, **35**, 1216–1217.

4 J. Wang, L. Wan, J. Chen and J. Yan, *Appl. Surf. Sci.*, 2015, **346**, 388–393.

5 (*a*) L. Weber and R. Tavangar, *Mater. Sci. Forum*, 2009, **59**, 111–115; (*b*) R. Tavangar, J. M. Molina and L. Weber, *Scr. Mater.*, 2007, **56**, 357–360; (*c*) K. Mizuuchi, K. Inoue, Y. Agari, M. Sugioka, M. Tanaka, T. Takeuchi, M. Kawahara, Y. Makino and M. Ito, *Composites, Part B*, 2012, **43**, 1445–1452.

6 (*a*) A. M. Abyzov, S. V. Kidalov and F. M. Shakhov, *J. Mater. Sci.*, 2011, **46**, 1424–1438; (*b*) A. M. Abyzov, F. M. Shakhov, A. I. Averkin and V. I. Nikolaev, *Mater. Des.*, 2015, **87**, 527–539; (*c*) K. Raza and F. A. Khalid, *J. Alloys Compd.*, 2014, **615**, 111–118; (*d*) C. Zhao and J. Wang, *Mater. Sci. Eng., A*, 2013, **588**, 221–227.

7 (*a*) R. Paul, S. Hussain, S. Majumder, S. Varma and A. K. Pal, *Mater. Sci. Eng., B*, 2009, **164**, 156–164; (*b*) R. Paul, S. Hussain and A. K. Pal, *Appl. Surf. Sci.*, 2009, **255**, 8076–8083; (*c*) W. C. Lan, S. F. Ou, M. H. Lin, K. L. Ou and M. Y. Tsai, *Ceram. Int.*, 2013, 4099–4104; (*d*) H. W. Choi, R. H. Dauskardt, S. C. Lee, K. R. Lee and K. H. Oh, *Diamond Relat. Mater.*, 2008, **17**, 252–257; (*e*) A. Pardo, C. J. Gómez-Aleixandre, P. Celis and J. G. Buijnsters, *Surf. Coat. Technol.*, 2012, **206**, 3116–3124; (*f*) H. W. Choi, J. H. Choi, K. R. Lee, J. P. Ahn and K. H. Oh, *Thin Solid Films*, 2007, **516**, 248–251.

8 (*a*) H. Tokura and M. Yoshikawa, *J. Mater. Sci.*, 1989, **24**, 2231–2238; (*b*) A. S. Barnard and M. Sternberg, *Nanotechnology*, 2007, **18**, 025702, (11pp).

9 (*a*) N. J. Pipkin, *J. Mater. Sci.*, 1980, **15**, 1755–1764; (*b*) F. K. de Theije, O. Roy, N. J. Van der Laag and W. J. P. Van Enckevort, *Diamond Relat. Mater.*, 2000, **9**, 929–934; (*c*) Z. Shpilman, I. Gouzman, E. Grossman, L. Shen, T. K. Minton, J. T. Paci, G. C. Schatz, R. Akhvlediani and A. Hoffman, *J. Phys. Chem. C*, 2010, **114**, 18996–19003.

10 (*a*) S. Sun, *Nanoscale*, 2015, **7**, 10850–10882; (*b*) C. G. Read, E. M. P. Steinmiller and K.-S. Choi, *J. Am. Chem. Soc.*, 2009, **131**, 12040–12041.

11 (*a*) T. Ohno, K. Sarukawa and M. Matsumura, *New J. Chem.*, 2002, **26**, 1167–1170; (*b*) L. Wu, J. Xing, Y. Hou, F. Y. Xiao, Z. Li and H. G. Yang, *Chem. – Eur. J.*, 2013, **19**, 8393–8396; (*c*) G. Liu, J. C. Yu, G. Q. Lu and H.-M. Cheng, *Chem. Commun.*, 2011, **47**, 6763–6783.

12 C. Liu, X. Han, S. Xie, Q. Kuang, X. Wang, M. Jin, Z. Xie and L. Zheng, *Chem. – Asian J.*, 2013, **8**, 282–289.

13 J. Yan, G. Wu, W. Dai, N. Guan and L. Li, *ACS Sustainable Chem. Eng.*, 2014, **2**, 1940–1946.

14 L. Yang, H. Jiang, W. Wang, D. Chu, J. Yang, M. Zhang, J. Lv, B. Wang, G. He and Z. Sun, *CrystEngComm*, 2016, **18**, 496–503.

15 (*a*) S. E. Habas, P. Yang and T. Mokari, *J. Am. Chem. Soc.*, 2008, **130**, 3294–3295; (*b*) H. Schlicke, D. Ghosh, L.-K. Fong, H. L. Xin, H. Zheng and A. P. Alivisatos, *Angew. Chem., Int. Ed.*, 2013, **52**, 980–982.

16 F.-R. Fan, Y. Ding, D. Y. Liu, Z. Q. Tian and Z. L. Wang, *J. Am. Chem. Soc.*, 2009, **131**, 12036–12037.

17 (*a*) T. Kondo, K. Hirata, T. Kawai and M. Yuasa, *Diamond Relat. Mater.*, 2011, **20**, 1171–1178; (*b*) T. Kondo, S. Aoshima, K. Hirata, K. Honda, Y. Einaga, A. Fujishima and T. Kawai, *Langmuir*, 2008, **24**, 7545–7548.

18 (*a*) M. Tsukada, S. Tsuneyuki and N. Shima, *Surf. Sci.*, 1985, **164**, L811–L818; (*b*) T. Halicioglu, *Surf. Sci.*, 1991, **259**, L714–L718; (*c*) J.-M. Zhang, H. Y. Li, K. W. Xu and V. Ji, *Appl. Surf. Sci.*, 2008, **254**(13), 4128–4133.

19 F. R. Marciano, L. F. Bonetti, R. S. Pessoa, M. Massi, L. V. Santos and V. J. Trava-Airoldi, *Thin Solid Films*, 2009, **517**, 5739–5742.

20 Y. Wu, Y. Liu, H. Li, J. Chen, S. Yu, B. Zhou and B. Tang, *Tribol. Int.*, 2016, **101**, 395–401.

21 N. Severin, S. Kirstein, I. M. Sokolov and J. P. Rabe, *Nano Lett.*, 2009, **9**, 457–461.

22 A. S. Barnard and M. Sternberg, *J. Mater. Chem.*, 2007, **17**, 4811–4819.

